Towards Broadly Optimum Multi-Core Fiber Designs

Joan M. Gené [1,2*], ***Peter J. Winzer*** [1], ***Haoshuo Chen*** [1], ***Roland Ryf*** [1],
Tetsuya Hayashi [3] ***and Takashi Sasaki*** [4]

[1] *Nokia Bell Labs, 791 Holmdel Rd, Holmdel, 07733, NJ, USA*
[2] *Universitat Politècnica de Catalunya, Jordi Girona 1-3, Barcelona, 08034, Spain*
[3] *Sumitomo Electric Industries, Ltd., 1 Taya-cho, Sakae-ku, Yokohama 244-8588, Japan*
[4] *Innovation Core SEI, Inc., 2355 Zanker Road, San Jose, CA 95131, USA*
**joan.gene@nokia-bell-labs.com*

Keywords: Coherent detection, channel capacity, crosstalk, fiber nonlinearity, space-division multiplexing.

Abstract

We show that key multi-core fiber (MCF) design parameters depend only weakly on the application scenario, from data-center interconnects to submarine links, leading to transmission-distance-independent optimum MCF designs. We analyse the dependence of the optimum MCF core count on fiber diameter and effective core area.

1. Towards Multi-Core Fiber Standardization

Space-division multiplexing (SDM) is widely recognized as a key technique to scale network capacities [1]. The first technological step beyond the use of conventional fiber bundles may be multi-core fiber (MCF) [2], initially using *nominally uncoupled cores* to avoid multiple-input-multiple-output digital signal processing (MIMO-DSP). A plethora of MCF types has been investigated over the past decade, but the many degrees of freedom in MCF design as well as the perceived application dependence of key design parameters has so far prevented MCF standardization as an important step towards volume manufacture, cost reduction, and deployment. As a step towards finding common grounds for standardization in the vast MCF design parameter space, it has recently been shown [3] that maximum MCF transmission capacities are achieved for a fairly universal value of core-to-core crosstalk (XT) per unit length, one of the most important MCF design parameters. Notably, this XT value was shown to be almost *independent of transmission reach*, from 100-km data-center interconnects to 10,000-km submarine links, in the context of modern optical transponders that use capacity-adaptation techniques such as probabilistic constellation shaping (PCS). The relative universality of core-to-core XT further results in an optimum number of cores for a given MCF outer diameter (OD) and, once an OD is agreed upon, pins down the MCF core geometry, a minimum requirement to directly interconnect and splice MCFs from different fiber manufacturers. This paper builds upon our previous analysis [3] and examines the optimum number of cores for various ODs, as well as the impact of the effective core area on capacity-optimum MCF designs.

2. MCF Capacity Optimization

The spectral efficiency (SE) per MCF core of a polarization-multiplexed transmission system using adaptive modulation such as PCS and Nyquist pulse shaping is given by [3] ,[4]

$$SE = 2 \cdot log_2\left(1 + \frac{1}{\eta_{TRX}} \frac{P_S}{\left(\eta_L P_{ASE} + \chi P_S^3 + \kappa P_S\right)}\right) \qquad (1)$$

where P_S denotes the per-channel (dual-polarization) signal launch power, and P_{ASE} is the amplified spontaneous emission (ASE) power within the signal channel's bandwidth. We consider both ideal distributed amplification [5] and lumped amplification with 80-km spans and a 5-dB optical amplifier noise figure (NF). Nonlinear interference noise (NLIN) is quantified by the parameter χ [6], [7], and κ denotes the *aggregate XT* experienced by a core from signals co-propagating at the same wavelength in all other cores. Note that expressing XT in multiples of P_S, does *not* necessarily imply equal signal powers in each core, although it turns out that the capacity-optimum signal power (for identical MCF cores) is XT-independent [3], [4], [8], [9], which results in all cores conveniently using the same signal power, irrespective of XT differences from a core's location within the MCF. In the *low core-to-core coupling regime* (i.e., MIMO-free transmission) which we exclusively consider, XT is modelled as additive white Gaussian noise [4], [10], and κ increases linearly with distance [2]; interactions of XT and fiber nonlinearities can be neglected. Transceiver implementation penalties are captured by η_{TRX} .

Figure 1 shows an exemplary MCF geometry, illustrating key parameters such as OD, outer cladding thickness (OCT), core pitch (Λ), and the refractive index profile of a trench-assisted core [11]. To compute the aggregate SE of a particular core-count MCF, we use *circle-packing theory* to determine a

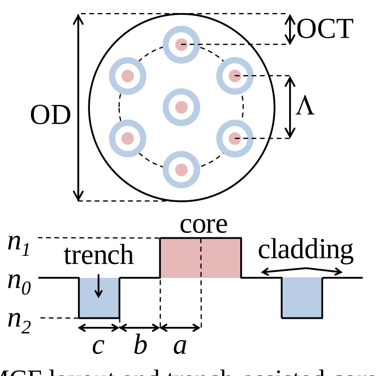

Fig. 1: MCF layout and trench-assisted core profile.

tightly-packed (typ. irregular) core lattice [12], [13] and calculate core-to-core XT using the analytical formulas provided in [11]. Attempts to further optimize the core locations based on the aggregate MCF capacity instead of the minimum core distance did not noticeably improve capacity. We conservatively assume an OCT of 30 µm [14] and trench-assisted cores ($a = b = c = 4.5\ \mu m$) [11], with -0.35% cladding-trench relative refractive index difference Δ_2 and $\Delta_{1,2} \cong (n_{1,2} - n_0)/n_{1,2}$. These parameters yield single-mode operation at the reference wavelength of 1550 nm. When varying the effective core area (Sec. 3.2) we modify Δ_1 between 0.2% and 0.9% to keep the normalized frequency (V-number) constant such as to guarantee single-mode operation in all considered cases.

3. Optimum Number of Cores

3.1 Outer Cladding Diameter (OD)

Figure 2 (a) shows the evolution of the aggregate SE, i.e., the sum of the (typ. different) SEs of the individual fiber cores, for three transmission distances (100 km, 1,000 km, 10,000 km) and three ODs (125 µm, 200 µm, 260 µm). For a given OD, the aggregate SE increases linearly with core count as long as XT is negligible (black dotted lines) and decreases once XT becomes dominant. The larger the OD, the more cores can be accommodated at the expense of the fiber's structural reliability [14] as well as more stringent angular alignment tolerances at connectors and splices [15]. Importantly, for a fixed OD the *optimum number of cores is almost the same for all transmission distances* [3]: The optimum numbers of cores for the three ODs are {4}, {12-14} and {23-26} across all relevant transmission distances. The average aggregate XT is shown in Fig. 2(b). For the optimum number of cores, we always find XT values around -60 dB (referenced to 1 km of MCF) [3].

Figure 2 assumes MCFs with standard single-mode cores (attenuation $\alpha = 0.2\ \ dB/km$; chromatic dispersion D = 17 $ps/(nm \cdot km)$; nonlinearity $\gamma = 1.3\ \ 1/(W \cdot \text{km})$, i.e., an effective core area of A_{eff} = 80 µm^2), 100 wavelength- and polarization-division multiplexed 50-GBaud channels at 50-GHz spacing, ideal Nyquist spectra, and ideal Gaussian-shaped constellations. However, except for A_{eff}, whose impact is discussed in Sec. 3.2, none of these assumptions is critical in terms of the optimum number of MCF cores, which is the focus of this paper. Solid lines in Fig. 2 represent ideal distributed amplification. Various lumped amplification scenarios are captured by the shaded areas, whose lower edges correspond to 80-km spans and a 5-dB amplifier NF. The optimum number of cores changes only slightly for lumped amplification, with {4}, {13-14}, and {24-27} for the considered ODs. All curves assume a transceiver implementation penalty, η_{TRX} in Eq. (1), of 3 dB.

Figure 3(a) shows the optimum number of cores vs. OD. As above, solid curves represent distributed amplification and shaded regions reflect lumped amplification, again revealing a fairly narrow range in the optimum number of cores across a wide range of considered transmission scenarios. Figure 3(b) shows the corresponding aggregate SE at the optimum design points. Further relevant parameters in this context are the *core density* (number of cores per unit area) and the *spatial SE* (SE per unit area [12], [16]). Core density and spatial SE in our

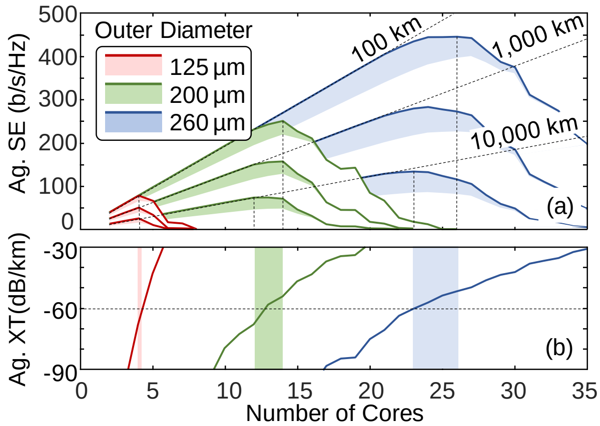

Fig. 2: Aggregate SE (a) and average aggregate XT for 1 km of MCF (b) vs. number of cores for ODs of 125 µm (red), 200 µm (green), and 260 µm (blue). Solid lines: Ideal distributed amplification. Shaded regions: Lumped amplification up to 80-km spans and 5-dB NF. Dotted black lines: XT-free reference. All cases: $\eta_{TRX} = 3\ dB$.

examples increase by 50% and 40%, respectively, when going from an OD of 125 µm to an OD of 300 µm due to better core packing (less wasted area) as the number of cores increases.

3.2 Effective Core Area (A_{eff})

Reducing the effective core area is another way to accommodate more cores within a MCF, with a trade-off between XT, NLIN, and loss when varying A_{eff} that is non-trivial [12], [16]: While the optimal balance between ASE and NLIN variances

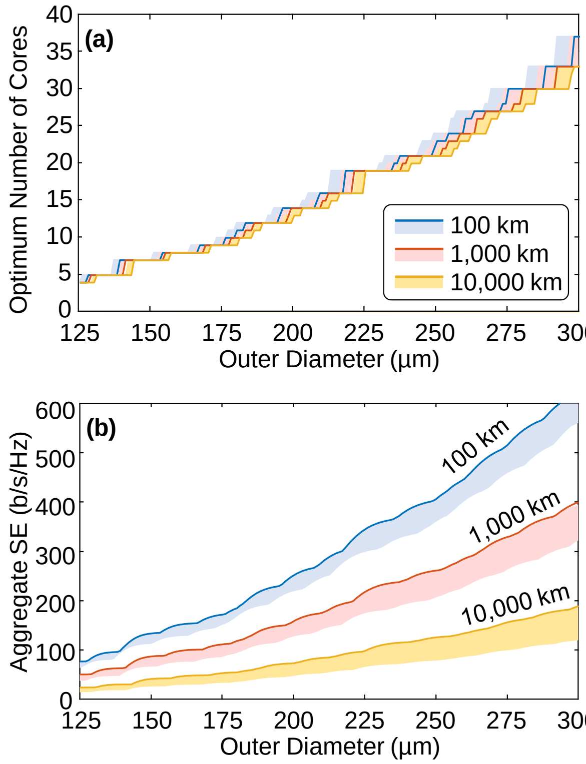

Fig. 3 (a) Optimum number of cores and (b) aggregate SE vs. outer cladding diameter. Solid curves: ideal distributed amplification. Shaded regions: Lumped amplification up to 80-km spans and 5-dB NF.

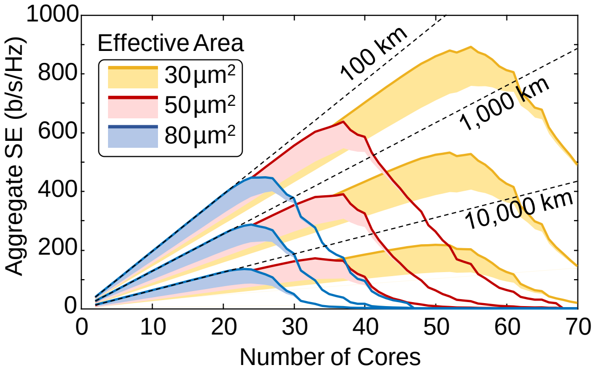

Fig. 4 Aggregate SE vs. number of cores for several effective core areas. Solid curves: ideal distributed amplification. Shaded regions: Lumped amplification up to 80-km spans and 5-dB NF. Dashed black lines show the XT-free case for reference. OD = 260 µm.

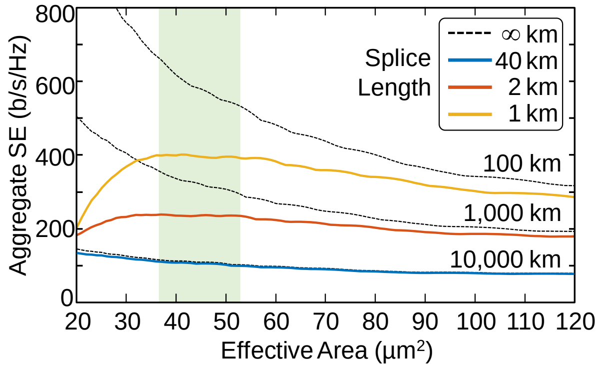

Fig. 5 Aggregate SE vs. A_{eff} assuming different splicing distances for each transmission reach. Dashed black lines: zero-splice-loss case. Lumped amplification with 80-km span lengths and 5-dB NF. OD = 260 µm.

is always 2:1 [6], [7], it can be shown using the results of [3] that the optimal ratio of ASE : NLIN : XT powers is

$$P_{ASE} : P_{NLIN} : P_{XT} = 2:1:3\kappa SNR_0 \ , \qquad (2)$$

with SNR_0 being the signal-to-noise ratio involving only ASE and NLIN. As κ and SNR_0 scale close-to-linear with transmission distance, the ratio of noise powers is almost distance-independent, corroborating the notion of distance-independent MCF designs. Figure 4 shows the aggregate SE vs. number of cores, with the effective core area as a parameter, ranging from 30 µm^2 to 80 µm^2. The OD is kept fixed at 260 µm (10^{-7} failure probability for 100 turns, 20 years, and a 1% proof level for a bending radius of 70 mm [14]). To re-scale the effective core area, we changed the core radius a ($A_{eff} \propto a^2$ with high accuracy) and re-scaled the size of the inner cladding b and the trench c to maintain $a = b = c$, cf. Fig. 1. To keep the same core propagation properties (same V-number), we adapted the core-cladding relative index. Once again, we see from Fig. 4 that for a given effective core area, the optimum number of cores is *fairly independent of transmission distance*. The change in slope of the curves in the XT-free region (dotted black lines) is small because the quadratic NLIN reduction with A_{eff} only reduces the SE *logarithmically*, cf. Eq. (1). On the other hand, a reduction in A_{eff} has an exponentially decreasing impact on XT [11] and, much more importantly, enables an increase in the number of cores for a fixed OD, which appears as a pre-log factor in the overall MCF capacity and consequently provides an *almost linear* benefit to the overall MCF capacity. Therefore, lowering the effective core area increases the MCF capacity (with full consideration of NLIN) until the capacity increase from a reduced A_{eff} is counter-balanced by some other capacity-reducing effect.

The most evident counter-balancing effect is additional loss due to too small effective core areas, most notably from an increased splice loss at low A_{eff} for a fixed lateral splice alignment accuracy. We therefore assume a lateral splicing accuracy of 0.8 µm, leading to a typical 0.1-dB splice loss for an 80-µm^2 effective area [17]. While submarine cables may only employ very few (if any) splices per span, terrestrial long-haul links are typically deployed in spliced sections of ~2 km. Metro fiber and data-center interconnects may use even shorter segments of, e.g., 1 km, for the thicker, higher-fiber-count cables used in such applications. Figure 5 shows the aggregate SE assuming lumped amplification and the above splicing assumptions for an MCF with a 260-µm OD. (For the trans-oceanic link we assumed splicing only at the repeaters, i.e., 2 splices every 80 km, equivalent to 1 splice every 40 km). It can be seen that under these realistic deployment assumptions, a fairly distance-independent optimal effective core area of 40-50 µm^2 is obtained. Slightly larger effective core areas may prove optimal when including additional losses from imperfect *rotational* MCF splice alignment, the influence of cleave angles, and increased *component XT* from fan-in/fan-out devices at low A_{eff} [15], [18].

4. Discussion and Conclusion

We determined the optimum number of cores in an MCF in the context of modern coherent systems using adaptive transponders. We showed that the optimum core count is virtually distance-independent, from 100-km data-center interconnects to 10,000-km submarine links. We also investigated the dependence of the optimum core count on cladding diameter and effective core area, yielding, again, reasonably distance-independent MCF designs. We finally note that MCFs designed for advanced coherent systems using the methodology presented here will also be able to support shorter-reach systems (1 to 100-km) based on intensity-modulation and direct-detection (IM-DD) with various pulse amplitude modulation (PAM) formats, as the ~60-dB/km XT values identified in Fig. 2 (~50 dB/10 km, ~40 dB/100 km) are sufficient for PAM [19], even when considering statistical XT variations that necessitate ~5 dB of extra margin to avoid system outages (10^{-5} outage probability) [10], [20]. Our results consequently narrow the vast design space of MCFs significantly and may contribute towards a consensus in MCF standardization.

Acknowledgment: This work was in part supported by the Spanish Ministry of Science, Innovation and Universities (ALLIANCE project TEC2017-90034-C2-2-R).

5. References

[1] P. J. Winzer, D. T. Neilson, and A. R. Chraplyvy, “Fiber-optic transmission and networking: The previous 20 and the next 20 years [Invited],” *Opt. Express*, vol. 26, no. 18, p. 24190, 2018.

[2] K. Saitoh, “Multicore fiber technology,” *J. Light. Technol.*, vol. 34, no. 1, pp. 55–66, Jan. 2015.

[3] J. M. Gene and P. J. Winzer, “A universal specification for multicore fiber crosstalk,” *IEEE Photonics Technol. Lett.*, vol. TBD, no. TBD, p. TBD, 2019.

[4] T. Hayashi, T. Taru, O. Shimakawa, T. Sasaki, and E. Sasaoka, “Uncoupled multi-core fiber enhancing signal-to-noise ratio,” *Opt. Express*, vol. 20, no. 26, p. B94, Dec. 2012.

[5] R.-J. Essiambre, G. Kramer, P. J. Winzer, G. J. Foschini, and B. Goebel, “Capacity Limits of Optical Fiber Networks,” *J. Light. Technol.*, vol. 28, no. 4, pp. 662–701, 2010.

[6] P. Poggiolini *et al.*, “The GN-model of fiber non-linear propagation and its applications,” *J. Light. Technol.*, vol. 32, no. 4, pp. 694–721, Feb. 2014.

[7] R. Dar, M. Feder, A. Mecozzi, and M. Shtaif, “Accumulation of nonlinear interference noise in fiber-optic systems,” *Opt. Express*, vol. 22, no. 12, p. 14199, Jun. 2014.

[8] R. Soares Luís *et al.*, “Spectral efficiency in crosstalk-impaired multi-core fiber links,” *Opt. Data Sci. Trends Shap. Futur. Photonics*, vol. 1055102, no. February, p. 1, Feb. 2018.

[9] D. J. Elsonf *et al.*, “Impact of intercore crosstalk on achievable information rates,” *IEEE Photonics Soc. Summer Top. Meet. Ser. SUM 2018*, pp. 21–22, 2018.

[10] T. Hayashi, T. Sasaki, and E. Sasaoka, “Behavior of inter-core crosstalk as a noise and its effect on Q-factor in multi-core fiber,” *IEICE Trans. Commun.*, vol. E97–B, no. 5, pp. 936–944, 2014.

[11] F. Ye, J. Tu, K. Saitoh, and T. Morioka, “Simple analytical expression for crosstalk estimation in homogeneous trench-assisted multi-core fibers,” *Opt. Express*, vol. 22, no. 19, p. 23007, Sep. 2014.

[12] T. Hayashi and T. Sasaki, “Design strategy of uncoupled multicore fiber enabling high spatial capacity transmission,” *2013 IEEE Photonics Soc. Summer Top. Meet. Ser. PSSTMS 2013*, vol. 4, no. 3, pp. 78–79, 2013.

[13] R. S. Luís *et al.*, “On the spectral efficiency limits of crosstalk-limited homogeneous single-mode multi-core fiber systems,” *Adv. Photonics 2017 (IPR, NOMA, Sensors, Networks, SPPCom, PS)*, vol. 2017, pp. 5–7, Jul. 2017.

[14] S. Matsuo *et al.*, “High-spatial-multiplicity multicore fibers for future dense space-division-multiplexing systems,” *J. Light. Technol.*, vol. 34, no. 6, pp. 1464–1475, 2016.

[15] Y. Amma, K. Takenaga, S. Matsuo, and K. Aikawa, “Fusion splice techniques for multicore fibers,” *Opt. Fiber Technol.*, vol. 35, pp. 72–79, Feb. 2017.

[16] T. Nakanishi, T. Hayashi, O. Shimakawa, and T. Sasaki, “Spatial-spectral-efficiency-enhanced multi-core fiber,” in *Optical Fiber Communication Conference*, 2015, p. Th3C.3.

[17] D. Marcuse, “Loss analysis of single-mode fiber splices,” *Bell Syst. Tech. J.*, vol. 56, no. 5, pp. 703–718, May 1977.

[18] O. Shimakawa, H. Arao, M. Harumoto, T. Sano, and A. Inoue, “Compact multi-core fiber fan-out with GRIN-lens and micro-lens array,” in *Optical Fiber Communication Conference*, 2014, p. M3K.1.

[19] G. Nicholl and C. Fludger, “Update on technical feasibility for PAM modulation,” *IEEE 802.3 NG100GE PMD Study Group*. [Online]. Available: http://www.ieee802.org/3/100GNGOPTX/public/mar12/plenary/nicholl_01b_0312_NG100GOPTX.pdf.

[20] B. J. Puttnam *et al.*, “Impact of intercore crosstalk on the transmission distance of QAM formats in multicore fibers,” *IEEE Photonics J.*, vol. 8, no. 2, pp. 1–9, Apr. 2016.